JURNAL KIMIA MULAWARMAN
Vol 21, No. 2, Mei 2024 pp. 84-92
https://jurnal.kimia.fmipa.unmul.ac.id/index.php/JKM
P-ISSN 1693-5616 E-ISSN 2476-9258

Synthesis and Characterization of Copper(II) Oxide (CuO-NP) Nanoparticles using Chemical Precipitation Method

Charlena[a,*], Sri Sugiarti[a], Dila Ardiansyah[a]

[a] Department of Chemistry, Faculty of Mathematics and Natural Science, Institut Pertanian Bogor, Bogor, Indonesia.
* Corresponding Author: charlena@apps.ipb.ac.id

ABSTRACT

This study aims to optimize the calcination temperature and see the effect of adding surfactant on the bandgap, particle size, crystallinity level of CuO nanoparticles (CuO-NP), and the activity of CuO nanoparticles as an antibacterial agent. CuO-NP was successfully synthesized using the chemical precipitation method with variations in calcination temperature of 400, 600, and 800 °C with NaOH as a precipitating agent. The synthesized nanoparticles were further characterized using a UV-Vis, XRD, and SEM-EDX spectrophotometer. The value of the CuO-NP bandgap increases with increasing temperature. The bandgap gets bigger when the absorbance value gets smaller. Increasing the calcination temperature causes the crystal size of CuO-NP to become larger. The best level of crystallinity of CuO-NP was obtained at 68,31% with a calcination temperature of 600 °C. Adding 1% PVP did not significantly prevent agglomeration between CuO-NP particles, thereby increasing the size of CuO-NP particles

OPEN ACCESS

Article History
Received 2023-07-14
Revised 2024-01-04
Accepted 2024-02-19

Keywords
Bandgap
CuO-NP
PVP
Temperature

1. Introduction

At the end of 2019, the world was shocked by the identification of a new virus called severe acute respiratory syndrome coronavirus-2 (SARS-CoV-2), commonly called COVID-19. The COVID-19 virus can infect the respiratory tract. The use of masks is, of course, highly recommended as an effort to prevent transmission from infected people but is not clinically detected [1]. The filtration power of masks can be increased by adding metal oxide components on the nanometer scale (nanoparticles). Some metal oxide nanoparticles have antibacterial [2] and antiviral [3] activities. Metal oxide nanoparticles that can be used as antibacterial and antiviral agents are TiO_2, ZnO, CuO, and MgO nanoparticles. Besides functioning as antibacterial and antiviral agents, nanoparticles can also be widely applied in sensors, bio-medical, catalysts, agriculture, electronics, and energy [4].

Nanoparticle synthesis is done to modify the particle size to a nanometer scale size of less than 100 nm so that similar bulk materials can produce different properties and functions [5]. Nano-sized materials will have specific characteristics that depend on their size, distribution, morphology and phase [6]. Copper(II) oxide (CuO) nanoparticles are one of the many metal oxide compounds that have been synthesized because they have the characteristics of a *p*-type semiconductor, have a monoclinic structure, have a reasonably narrow energy band gap of around 1,2 eV [7], and have good catalytic activity and selectivity [8]. CuO nanoparticles are widely used because they are cheaper than silver or other metal nanoparticles. CuO nanoparticles can be produced by chemical synthesis in the laboratory.

The methods commonly used to synthesize copper nanoparticles are chemical and physical. The processes of the two ways include electrochemical, hydrothermal, sol-gel, chemical

reduction [9], photochemical reduction, the addition of surfactant agents, capping agents, vacuum impregnation [10], thermal decomposition [11], and precipitation methods [12]. The synthesis of copper oxide nanoparticles in this study was carried out using chemical precipitation methods. The chemical precipitation method was chosen because it has a relatively easy synthesis step and tends to operate in one step. The temperature parameter is a parameter that can affect the product to be produced. An increase in temperature can affect the purity and size of the resulting particles. The calcination process is a process that has an essential role in producing nanocrystals which is expected because it can make crystals with high purity. Luna *et al*. (2015) [8] reported that at a calcination temperature of 600 °C, the crystalline degree phase of the monoclinic CuO-NP phase was nearly perfect.

The tendency of agglomeration will form as the temperature increases; adding surfactants can be a solution to prevent agglomeration. One of the surfactants that can be used is polyvinyl pyrrolidone (PVP). Surfactants can be used as a steric barrier, thereby minimizing the occurrence of agglomeration. The calcination temperature that will be applied during the synthesis is modified to produce a product with the best results and properties with various temperature variations starting from 400, 600, and 800 °C. The resulting copper oxide nanoparticles will be further characterized using UV-Vis, XRD, and SEM-EDX. This study aims to optimize the calcination temperature in the synthesis of copper(II) oxide (CuO-NP) nanoparticles using the chemical precipitation method, to characterize CuO nanoparticles, to observe the effect of adding surfactant on gap energy, particle size, and crystallinity of CuO nanoparticles.

2. Research Methodology

2.1. Tools and Materials

The tools used in this study were glassware, a set of centrifuges, a set of UV-Vis spectrophotometry instruments (U-2800 Spectrophotometer), a set of X-ray diffractometer instruments (XRD Empyrean Series 3 Panalytical), a set of scanning electron microscopy instruments with energy dispersive X-ray (Thermo Scientific Quarta 650), and OriginPro 8.5 software. The materials used in the research, namely $CuCl_2{\cdot}2H_2O$ (Pudak); NaOH 3 M (Merck); PVP 1% (w/v); $(NH_4)_2CO_3$ 0,1 M (Merck), Mueller–Hinton agar (Merck), *S. aureus*, and aquadest

2.2. Synthesis of Copper(II) Oxide Nanoparticles Without and With the Addition of PVP Surfactants (Modification of Luna *et al*. 2015 [8])

The synthesis was carried out according to the method of Luna *et al*. (2015) [8] modified. In the first step, 9 g of copper(II) chloride dihydrate ($CuCl_2{\cdot}2H_2O$) was weighed and dissolved in 50 mL of distilled water with constant stirring using a magnetic stirrer for 30 minutes. 3 M NaOH has added as much as 50 mL into the $CuCl_2{\cdot}2H_2O$ solution drop by drop with continuous stirring and heat until the color changed from blue to black; the reaction was allowed to proceed with stirring for 90 minutes at room temperature. The resulting precipitate was centrifuged to separate the solid and liquid phases at 5000 rpm for 20 minutes. Furthermore, the precipitate is washed with distilled water 3–4 times to remove the salt that is still contained in the precipitate. The final product is dried in an oven at 105 °C for 4 hours. Samples were calcined at 400, 600, and 800 °C in a furnace for 4 hours to compare results. After cooling, the product is stored in a desiccator. This procedure was also carried out to synthesize CuO nanoparticles by adding PVP surfactant. The process ends with the characterization of the synthesis product using UV-Vis, XRD, and SEM EDX.

3. Result and Discussion

3.1. Copper(II) Oxide Nanoparticles (CuO-NP)

Copper nanoparticles are one of the metal nanoparticles widely used in the pharmaceutical field because they have antibacterial, antioxidant [2], and antiviral [3] activities in the form of metal and oxides. Copper oxide has two crystalline phases: cuprous oxide (Cu_2O) and cupric oxide (CuO). Synthesis of CuO nanoparticles was carried out using the chemical precipitation method. The chemical precipitation method was chosen because it has a simple reaction step

with the basic principle of material deposition with the help of a precipitating agent. The precursor $CuCl_2 \cdot 2H_2O$ is used as the base material for copper. CuO nanoparticles are formed by the decomposition of $CuCl_2 \cdot 2H_2O$ precursors into $Cu(OH)_2$ when the solution has reached saturation point with the help of a precipitating agent. The precipitating agent can be an alkaline hydroxide base, such as KOH and NaOH. $Cu(OH)_2$ will decompose to CuO at around 80 °C.

The precipitation reaction can be seen visually when the green $CuCl_2 \cdot 2H_2O$ precursor solution changes colour slowly to blue, thickening, and gradually darkening to black as the reaction progresses. The description of the temperature when the reaction is taking place, will make the reaction go faster because the particles will decompose more quickly as the reaction temperature increases. The reaction for forming CuO nanoparticles with the initial precursor $CuCl_2 \cdot 2H_2O$ occurs based on the reaction equations (1) and (2).

$$CuCl_2 \cdot 2H_2O(aq) + 2NaOH(aq) \rightarrow Cu(OH)_2(s)\downarrow + 2NaCl(aq) \quad (1)$$

$$Cu(OH)_2(s) \rightarrow CuO(s) + H_2O(g) \quad (2)$$

CuO products were calcined at 400, 600, and 800 °C. Visually, the outcome of CuO nanoparticles after being calcined at 800 °C has different results with the same two treatments, as shown in Figure 1.

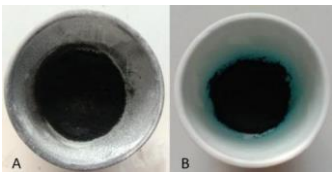

Fig 1. Calcination results of CuO nanoparticles at 800 °C without the addition of PVP (A) and the addition of PVP (B)

Product A in Figure 1 is a CuO nanoparticle, having the same results as product CuO-NP calcined at different temperatures. Product B, nanoparticles with the addition of PVP, looks like a blue color around the product in the crucible. The resulting blue color is presumably because the PVP structure used was damaged when the calcination temperature was increased to 800 °C, so it can be interpreted that the best temperature for making CuO nanoparticles with the addition of PVP is at a maximum temperature of 600 °C. Temperature plays an essential role in the purity and size of the resulting product. The higher the temperature, the better the level of product purity. According to the report by Luna et al. (2015) [8], an increase in calcination temperature will result in a larger particle size because it tends to undergo agglomeration.

Agglomeration can be prevented by adding surface-active compounds (surfactants) so that stabilization occurs during the reaction. Surfactants can be used as a steric barrier, thereby minimizing the occurrence of agglomeration. The surfactants used usually have hydrophilic heads and hydrophobic tails. The surface of the nanoparticles will absorb the hydrophilic portion of the surfactant, and the hydrophobic portion will provide steric repulsion to prevent agglomeration. The surfactant used in this study was polyvinyl pyrrolidone (PVP). The highly polar amide group of PVP will stick to the surface of the nanoparticles to protect against agglomeration.

3.2. UV-Vis Spectrum of Copper(II) Oxide Nanoparticles

Characterization using a UV-Vis spectrophotometer is expressed as a relationship curve between the wavelength (nm) and the absorbance value.

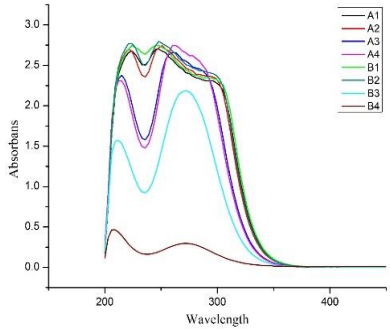

Fig 2. UV-Vis spectrum of CuO nanoparticles (A) and CuO·PVP (B) (A1;B1: temperature 105 °C, A2;B2: calcination temperature 400 °C, A3;B3: calcination temperature 600 °C, A4;B4: calcination temperature 800 °C)

Figure 2 shows the UV spectrum of all CuO nanoparticle samples treated at different calcination temperatures. Sample A is a CuO particle, and sample B is a CuO particle with the addition of PVP surfactant.

Table 1. Maximum wavelength of CuO nanoparticles

Samples	λmax (nm)
A1	248
A2	251
A3	263
A4	260
B1	245
B2	248
B3	272
B4	272

Based on the results obtained by testing using a UV-Vis spectrophotometer, the absorbance value and maximum wavelength value (λmax) of the CuO nanoparticles are known. The resulting λmax value varies from sample to sample (Table 1). There was a shift in λmax as the calcination temperature increased. The λmax shift occurs due to a change in the crystal size of the CuO nanoparticles. According to Rahayu *et al*. (2020) [13], an increase in λmax indicates an increasing size of nanoparticles, and vice versa; when the value of λmax falls, the size of the nanoparticles gets smaller. The data generated from the UV-Vis results can be used to find the energy bandgap of CuO nanoparticles. The bandgap is a particle's minimum energy to move or excite electrons from the valence band to the conduction band [14]. Bandgap values can be found using the tauc plot method. Based on Figure 3, the bandgap values of the resulting CuO samples are different and tend to experience an increase in bandgap values with increasing temperature.

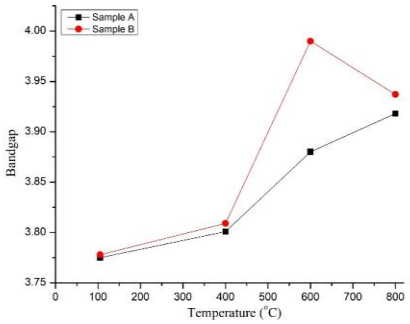

Fig 3. Relationship between temperatures and bandgap

Based on the results, the bandgap values of sample A and sample B are similar. There is an anomaly in the bandgap value of sample B4 (Table 2), where the resulting bandgap is smaller than the bandgap value of sample B3.

Table 2. Bandgap values on gap energy

Samples	Temperature (°C)	Gap Energy (eV)
CuO	105	3,775
CuO·PVP	105	3,778
CuO	400	3,801
CuO·PVP	400	3,809
CuO	600	3,880
CuO·PVP	600	3,990
CuO	800	3,918
CuO·PVP	800	3,937

This difference is generated because sample B4 has two plot peaks for bandgap values. The resulting two plot peaks are likely due to size and morphology, and the inhomogeneous sample B4 resulted in two dominant sizes. The difference in bandgap can be caused by the absorbance value obtained—the increase in calcination temperature results in a greater value of the resulting bandgap. The results of the bandgap values obtained are contrary to the theory, which states that the higher the temperature, the smaller the bandgap values because the particle size will increase with agglomeration. The increase in the bandgap value, as the calcination temperature increases, can occur due to the resulting quantum particle effect [15], the primary material for making nanoparticles, the resistivity of the material, and the quality of the product layer produced [16]. This can be caused by electrons that can move freely in the conduction band and accelerate CuO's conductivity [17]. Based on the results, it can be interpreted that the CuO nanoparticles in this study belong to an insulator-type material because the resulting bandgap is more than 3 eV, where the bandgap value of semiconductor materials ranges from 1–3 eV [18].

3.3. Diffractogram of Copper(II) Oxide Nanoparticles

Characterization using XRD is shown in Figure 3. The diffraction peaks indicated that the tested particle had a diffraction pattern distribution of CuO (tenorite) nanoparticles. The diffraction resulting from the three CuO samples tested is very visible, and each sample has diffraction characteristics that are not much different.

 ISSN 2476-9258

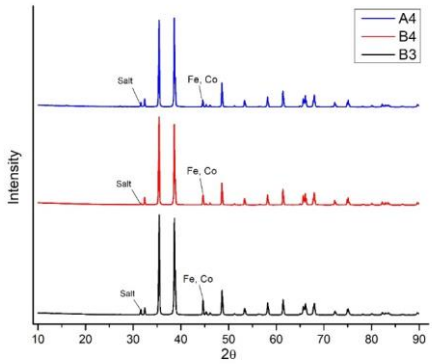

Fig 4. Diffractogram of CuO nanoparticles; (B3) CuO·PVP 600 °C, (B4) CuO·PVP 800 °C, (A4) CuO 800 °C

Each crystalline phase has its diffractogram arrangement and characteristics. The crystal structure formed can be identified by matching each peak that appears on the diffractogram with the Joint Committee Powder Diffraction Standard (JCPDS) data. Strong diffraction of CuO nanoparticles and Miller indices (*hkl*) was read on the diffractogram at an angle of 2θ 32,4° (110); 35,4° (111); 38,6° (111); 48,6° (202); 53,4° (020); 58,2° (202); 61,4° (113); 66,1° (311); 67,9° (220); and 75,1° (222). The diffraction read indicated that the CuO nanoparticles had a monoclinic structure (Figure 5) with a = 4,685; b = 3,423; and c = 5,132 according to data on JCPDS #41-0254 and #48-1548.

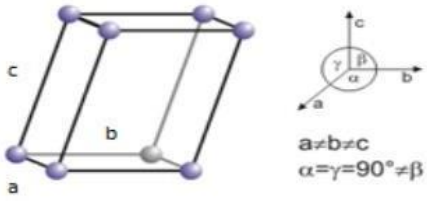

Commented [HS1]: is there any citation for the picture?

Fig 5. Monoclinic crystal structure [19]

From the diffractogram in Figure 4, there are diffraction patterns of impurities such as salt and metals such as iron (Fe) and cobalt (Co) which are read on the diffractogram with low intensity. Diffraction from contaminants that are read, the intensity decreases with increasing temperature. Crystal size apparent crystal size (ACS) uses the Debye–Scherrer equation. The ACS results of CuO nanoparticles are presented in Table 3.

Table 3. Apparent crystal size and crystallinity level of CuO nanoparticles

Sample	Temperature (°C)	Crystal Size (nm)	Crystallinity (%)
CuO·PVP	600	30,43	68,31
CuO·PVP	800	34,56	63,65
CuO	800	33,47	66,69

The results of ACS experienced an increase in crystal size along with the rise in the given calcination temperature. However, the results obtained are still on the nanoparticle scale and have the potential to be used as coatings for masks, which in the study of El-Nahhal *et al*. (2016) [20], CuO nanoparticles with a size of 50 nm were successfully coated on the surface of cotton and could fight bacteria well. The increase in crystal size is due to the agglomeration tendency of CuO nanoparticles. Agglomeration occurs because the crystallization rate of CuO nanoparticles increases rapidly, so the movement between particles becomes more reactive with increasing temperature [21].

Samples with a calcination temperature of 800 °C have different results. Sample B4 is a sample of CuO nanoparticles treated with the addition of PVP surfactant, which has a larger crystal size than sample A4 which is a sample of CuO nanoparticles. However, nanoparticles treated at 600 °C with the addition of PVP had smaller crystal sizes compared to CuO nanoparticles in the report by Luna *et al*. (2015) [8], in which the crystal size obtained was in the range of 32,5 nm with the same starting material and temperature treatment.

The best level of crystallinity of CuO nanoparticles was obtained in sample B3 at 600 °C. The level of crystallinity decreased at 800 °C calcination temperature. The decrease in the level of CuO crystallinity is due to the reduced intensity on the diffractogram. The level of crystallinity indicates that the arrangement of atoms in crystal particles has a regular and repeating shape in 3-dimensional space. Sample B3 is the sample that has the highest diffractogram intensity. According to Sundari *et al*. (2018) [22], the level of crystallinity with a high intensity of CuO nanoparticles will have reasonably good crystallinity.

3.4. Morphology of Copper(II) Oxide Nanoparticles

TDS adalah terlarutnya zat padat yang biasanya disebabkan oleh bahan anorganik berupa ion, senyawa, dan koloid di dalam air [22]. Hasil pengukuran TDS air gambut setelah proses adsorpsi ditampilkan pada Gambar 4.

The morphology of CuO nanoparticles was carried out using a scanning electron microscope (SEM) instrument. Figure 6 is the SEM result of a sample of CuO nanoparticles treated with a 600 °C calcination temperature.

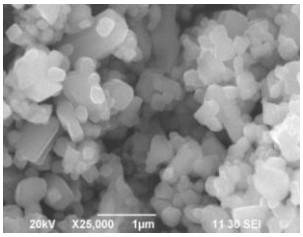

Fig 6. Morphology of CuO nanoparticles at calcination temperature 600 °C

SEM analysis was performed at 25000× magnification. The shape or morphology of the CuO nanoparticles looks similar to a monoclinic structure that is evenly distributed and has a uniform shape. The particle size obtained from the SEM results has large particle size, presumably due to the agglomeration of CuO nanoparticles. Agglomeration occurs due to buildup between particles caused by the absence of a steric barrier between particles when the temperature increases. The agglomeration tendency of each particle is shown in Figure 6, which can result in a larger particle size. The elemental composition of CuO nanoparticles was analyzed using energy dispersive X-ray (EDX). Figure 7 shows the EDX analysis of CuO nanoparticle samples treated with a 600 °C calcination temperature.

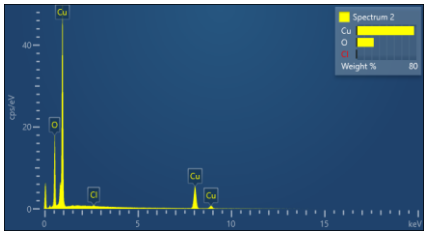

Fig 7. Elemental compositions of CuO nanoparticle

The results obtained indicate the presence of elements such as copper (Cu) and oxygen (O), which are the main constituents of CuO nanoparticles. Also, read the impurities as elemental chloride (Cl) with a minimal percentage. The percentage by weight of each element is obtained for a Cu atom of 76,81% with a weight of 1,032 keV; 22,99% O atoms with a weight of 0,231 keV; and for Cl atoms by 0,2% with a weight of 0,003 keV. The EDX results show a uniform distribution of atoms with a 1:1 ratio in CuO. These results indicate that the resulting nanoparticles have good purity because only a few impurities are detected in the CuO nanoparticles.

4. Conclusion

CuO nanoparticles have been successfully synthesized using chemical precipitation methods. The description of the calcination temperature resulted in a change in the characteristics of CuO-NP. The temperature of 600 °C is the best temperature to carry out the synthesis with the precipitation method. The crystal size of CuO-NP increases with increasing calcination temperature. The best crystallinity level of CuO-NP was produced at a calcination temperature of 600 °C. The trend of decreasing crystallinity level occurs when the temperature increases to 800 °C. Adding 1% PVP surfactant can produce smaller particle sizes than pure CuO-NP. However, it is not so significant in preventing agglomeration. Agglomeration with adding 1% PVP is only effective up to 600 °C but not at 800 °C.

References

[1] K. H. Chan and K.-Y. Yuen, "COVID-19 epidemic: disentangling the re-emerging controversy about medical facemasks from an epidemiological perspective," *International Journal of Epidemiology*, vol. 49, no. 4, pp. 1063–1066, Mar. 2020, doi: 10.1093/ije/dyaa044.

[2] A. K. Chatterjee, R. Chakraborty, and T. Basu, "Mechanism of antibacterial activity of copper nanoparticles," *Nanotechnology*, vol. 25, no. 13, p. 135101, Feb. 2014, doi: 10.1088/0957-4484/25/13/135101.

[3] P. Merkl, S. Long, G. M. McInerney, and G. A. Sotiriou, "Antiviral Activity of Silver, Copper Oxide and Zinc Oxide Nanoparticle Coatings against SARS-CoV-2," *Nanomaterials*, vol. 11, no. 5, p. 1312, May 2021, doi: 10.3390/nano11051312.

[4] K. S. Kavitha, S. Baker, D. Rakshith, H. U. Kavitha, B. P. Harini, and S. Satish, "Plants as Green Source towards Synthesis of Nanoparticles," *International Research Journal of Biological Sciences*, vol. 2, no. 6, pp. 66–76, Jun. 2013, [Online]. Available: http://www.isca.in/IJBS/Archive/v2/i6/14.ISCA-IRJBS-2013-048.pdf

[5] A. Masykuroh and H. Puspitasari, "Potensi tanaman keladi sarawak Alocasia macrorrhizos dalam biosintesis nanopartikel perak (NNP): analisis surface plasmon resonance (SPR) sebagai fungsi waktu," Bioma. Vol. 5, No. 2, pp. 233–240, 2020.

[6] Willems and V. D. Wildenberg, *"Roadmap Report on Nanoparticle*," Barcelona (ESP): W&W Españas, 2005.

[7] D. P. Singh and N. Ali, "Synthesis of TiO2 and CuO nanotubes and nanowires," *Science of Advanced Materials*, vol. 2, no. 3, pp. 295–335, Sep. 2010, doi: 10.1166/sam.2010.1095.

[8] I. Z. Luna, L. N. Hilary, A. M. S. Chowdhury, M. A. Gafur, N. Khan, and R. A. Khan, "Preparation and characterization of copper oxide nanoparticles synthesized via chemical precipitation method," *OAlib*, vol. 02, no. 03, pp. 1–8, Jan. 2015, doi: 10.4236/oalib.1101409.

[9] V. D. Kulkarni and P. S. Kulkarni, "Green Synthesis of Copper Nanoparticles Using Ocimum Sanctum Leaf Extract," *International Journal of Chemical Studies*, vol. 1, no. 3, pp. 01–04, Oct. 2013, [Online]. Available: https://www.chemijournal.com/vol1Issue3/sep2013/12.1.pdf

[10] F. S. Arakawa, Q. L. Shimabuku-Biadola, M. F. Silva, and R. Bergamasco, "Development of a new vacuum impregnation method at room atmosphere to produce silver–copper oxide nanoparticles on activated carbon for antibacterial applications," *Environmental Technology*, vol. 41, no. 18, pp. 2400–2411, Jan. 2019, doi: 10.1080/09593330.2019.1567607.

[11] M. Salavati-Niasari and F. Davar, "Synthesis of copper and copper(I) oxide nanoparticles by thermal decomposition of a new precursor," *Materials Letters*, vol. 63, no. 3–4, pp. 441–443, Feb. 2009, doi: 10.1016/j.matlet.2008.11.023.

[12] K. Phiwdang, S. Suphankij, W. Mekprasart, and W. Pecharapa, "Synthesis of CUO nanoparticles by precipitation method using different precursors," *Energy Procedia*, vol. 34, pp. 740–745, Jan. 2013, doi: 10.1016/j.egypro.2013.06.808.

[13] N. Rahayu, G. Gusrizal, and N. Nurlina, "Ekstrak Umbi Bawang Dayak (Eleutherine palmifolia (L.) Merr.) sebagai Pereduksi Ion Perak dalam Sintesis Nanopartikel Perak," *Indonesian Journal of Pure and Applied Chemistry*, vol. 3, no. 3, p. 17, Apr. 2021, doi: 10.26418/indonesian.v3i3.44151.

[14] D. Triwardiati and I. R. Ermawati, "Analisis Bandgap Karbon Nanodots (C-Dots) Kulit Bawang Merah Menggunakan Teknik Microwave," in Pros. SemNas. Teknoka, Vol. 3, pp. E25-E30, 2018. [Online]. Available: https://journal.uhamka.ac.id/index.php/teknoka/article/view/2810.

[15] T. H. Tran and V. T. Nguyen, "Copper Oxide nanomaterials Prepared by solution methods, some properties, and potential applications: A Brief review," *International Scholarly Research Notices*, vol. 2014, pp. 1–14, Dec. 2014, doi: 10.1155/2014/856592.

[16] N. H. Efendi, and H. Sutanto, "Pengaruh Temperatur Sintering terhadap Sifat Optik Lapisan Tipis Zinc Oxide (Zno) yang Dideposisi Diatas Substrat Kaca dan Aplikasinya untuk Mendegradasi Pewarna Methylene Blue," *Youngster Physics Journal*, vol. 3, no. 2, pp. 135-142, Apr. 2014. [Online]. Retrieved from : https://ejournal3.undip.ac.id/index.php/bfd/article/view/5286.

[17] A. Sedky, T. A. El-Brolossy, and S. B. Mohamed, "Correlation between sintering temperature and properties of ZnO ceramic varistors," *Journal of Physics and Chemistry of Solids*, vol. 73, no. 3, pp. 505–510, Mar. 2012, doi: 10.1016/j.jpcs.2011.11.035.

[18] M. M. Y. Missa, R. K. Pingak, and H. I. Sutaji, "Penentuan Celah Energi Optik Ekstrak Daun Alpukat (*Persea Americana Mill*) Asal Desa Oinlasi menggunakan Metode Tauc Plot," *Jurnal Fisika/Jurnal Fisika : Fisika Sains Dan Aplikasinya*, vol. 3, no. 1, pp. 86–90, Dec. 2018, doi: 10.35508/fisa.v3i1.606.

[19] G. L. Miessler, P. J. Fischer, and D. A. Tarr, *Inorganic chemistry 5th Ed,* US: Pearson Higher Ed, 2014, pp. 214-241.

[20] I. M. E. Nahhal, A. A. Elmanama, and N. M. Amara, "Synthesis of Nanometal Oxide–Coated Cotton composites," in *Cotton Research*, I. Y. Abdurakhmonov, Ed. InTech eBooks, 2016. doi: 10.5772/63505.

[21] A. D. Rosanti, A. R. K. Wardani, and H. A. Anggraeni, "Pengaruh Suhu Kalsinasi terhadap Karakteristik dan Aktivitas Fotokatalis N/Tio2 pada Penjernihan Limbah Batik Tenun Ikat Kediri," *Cakra Kimia (Indonesian E - Journal of Applied Chemistry)*, vol. 8, no. 1, pp. 26–33, May 2020, [Online]. Available: https://ojs.unud.ac.id/index.php/cakra/article/view/62801.

[22] C. D. D. Sundari, R. F. Rahayu, and N. Windayani, "Sintesis dan Karakterisasi Nanostruktur Tembaga Oksida dengan Metode Hidrotermal," *Al Kimiya: Jurnal Ilmu Kimia Dan Terapan*, vol. 5, no. 1, pp. 48–51, Dec. 2018, doi: 10.15575/ak.v5i1.3725.